Proceedings 10th NUMGE 2023
10th European Conference on Numerical Methods in Geotechnical Engineering
Zdravkovic L, Kontoe S, Taborda DMG, Tsiampousi A (eds)

https://doi.org/10.53243/NUMGE2023-321

3D numerical analysis of the interaction between the Jubilee and Northern Line tunnels at Waterloo

M. Stewart[1], A. Ruiz López[2] & A. Tsiampousi[2]
[1]*AKTII, London, UK (formerly Imperial College London)*
[2]*Department of Civil and Environmental Engineering, Imperial College, London*

ABSTRACT: A competent 3D numerical analysis is required for the detailed assessment of the potential damage of existing tunnels resulting from new tunnel construction. However, few case studies, particularly in London Clay, have been considered in the literature and the validity of 3D numerical analyses for the interaction between new and existing tunnels is yet to be established. In this paper, the construction of the Jubilee Line twin tunnels beneath the existing Northern Line tunnels at Waterloo is simulated numerically. A parametric study has been carried out to investigate the role of K_0 in modelling perpendicular twin tunnel interaction, considering both high and reduced K_0 conditions, with comparisons made against the empirical framework. To account for the presence of the joints, the existing tunnels adopted a reduced anisotropic lining stiffness. The numerical results were in good agreement with settlement measurements taken along the invert of the existing tunnels, with estimates being more accurate than the empirical framework.

Keywords: 3D finite element analysis; tunnelling; tunnel-tunnel interaction; London clay

1 INTRODUCTION

Excessive ground movements caused by tunnel construction pose a significant damage risk to nearby infrastructure. Displacement estimates typically rely on the methods detailed in Peck (1969) and Mair et al. (1993). These methods are empirical, limited to ground conditions similar to those used in their development and strictly applicable to greenfield conditions. The application of numerical methods overcomes all these limitations and offers a more sophisticated tool of analysis.

In regard to numerical predictions of tunnelling-induced ground movements in greenfield conditions, it is well established that simple linear elastic perfectly plastic soil models predict displacement profiles that are too wide and shallow (Guedes de Melo and Pereira, 2000). Franzius et al. (2005) also showed that predicting accurately the surface movements in high K_0 conditions is challenging even when adopting non-linear soil stiffness models.

For tunnel-tunnel interaction, most cases consider parallel scenarios that can be conveniently analysed in 2D plane strain as presented in Addenbrooke and Potts (1996; 2001). When assessing surface displacements caused by closely spaced parallel interaction, Addenbrooke and Potts (2001) predicted a non-symmetric settlement trough which is also observed in field observations (Mair and Taylor, 1997). When modelling a vertical "piggy-back" type scenario, Addenbrooke and Potts (1996) predicted a relationship of wider displacement profiles with decreasing pillar widths between tunnels.

Regarding previous investigations considering 3D perpendicular interactions, Liu et al. (2009) predicted surface heave which is considered unrealistic and caused by assuming soil linear elasticity along with high horizontal ground stresses. Avgerinos et al. (2017) investigated the interaction between two tunnels in London Clay, motivated by the construction of the Crossrail tunnels beneath the existing Central Line tunnels in central London. Significant geometric simplifications were however introduced preventing a meaningful comparison of the numerical predictions with field measurements. It is clear that further investigations studying 3D perpendicular tunnel interaction using advanced constitutive models are necessary.

In this paper, the construction of the Jubilee Line Extension (JLE) twin tunnels beneath the Northern Line (NL) tunnels at Waterloo International Terminal (WIT) is simulated numerically with PLAXIS 3D (Bentley, 2022). The numerical predictions are compared with precise levelling measurements undertaken along the NL tunnel inverts presented in Standing and Selman (2001). Given its significant effect on displacement estimations, the impact of two different K_0 profiles on the results are assessed. A comparison against the empirical framework to estimate subsurface displacements following the methods outlined in Mair et al. (1993) is also established.

2 THE LONDON WATERLOO SITE

Overview

Figure 1 depicts a plan detailing the alignment of several underground lines found at the WIT site. The Bakerloo Line and Waterloo and City Line tunnels were deemed sufficiently far, horizontally and vertically, from the NL tunnels and were not included in the model.

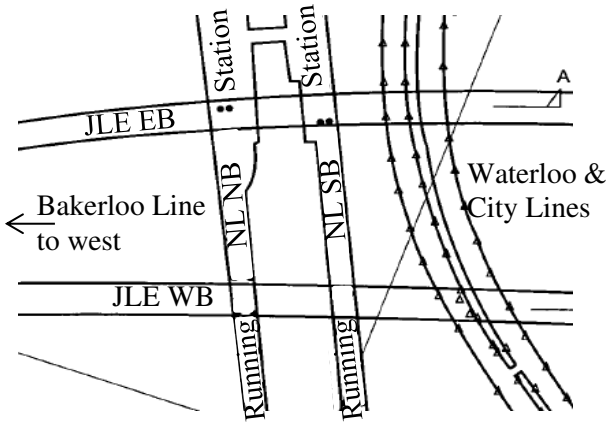

Figure 1. Plan detailing respective geometries of JLE and NL tunnels (Standing and Selman, 2001)

2.1 Tunnel details

Both sets of tunnels are formed within the London Clay Formation. The NL tunnels comprise both station and running North (NB) and South Bound (SB) tunnels. The JLE tunnels comprise the East (EB) and West Bound (WB) running tunnels. The extension of the NL to Waterloo was completed in 1923/24 while the JLE tunnels were constructed in 1994/95 (Standing and Selman, 2001). The external diameters of the NL station and running tunnels are approximately 6.68m and 3.57m respectively. The JLE external tunnel diameters are approximately 4.85m.

Segmental grey cast iron (GCI) linings were employed to build the NL tunnels. The tunnel segments comprised a skin and two circumferential flanges forming a U cross-section. The dimensions of the tunnel cross-sections were assumed to follow those of standard GCI linings of the London Underground.

The JLE tunnel lining thickness is 450mm comprising 150mm Sprayed Concrete Lining and 300mm cast-in-place concrete segments (Standing and Selman, 2001).

The inverts of the NL and JLE tunnels are located at depths of approximately 21.9m and 32.05m respectively. The vertical clearance between the JLE and NL tunnels is 5.3m. The axis to axis spacing of the JLE tunnels is 31.8m whereas that between the NL tunnels is approximately 12m.

2.2 Ground conditions

The ground conditions present on site are typical of those encountered in London and are based on records published on the BGS website. The soil profile comprises Made Ground (MG) to a depth of 4.6m overlying Terrace Gravels (TG) to a depth of 10.4m. Underlying the TG, London Clay (LC) is encountered to a depth of 39.6m and it is underlain by the Lambeth Group (LG) to 58.6m. Thanet Sands (TS) are assumed to underlie the LG to depths in excess of 68.8m, which is taken as the bottom of the model.

3 DESCRIPTION OF NUMERICAL MODEL

3.1 Geometry, boundary conditions and initial stresses

Figure 2 shows the geometry of the numerical model. In plan view, the model dimensions comprised approximately 159m by 250m parallel and perpendicular to the JLE tunnel axis respectively. These dimensions were chosen based on preliminary analyses where the impact of the model extent on the tunnelling-induced displacements was investigated (Stewart, 2022). Solid and shell elements were used to simulate the soil and tunnel linings, respectively.

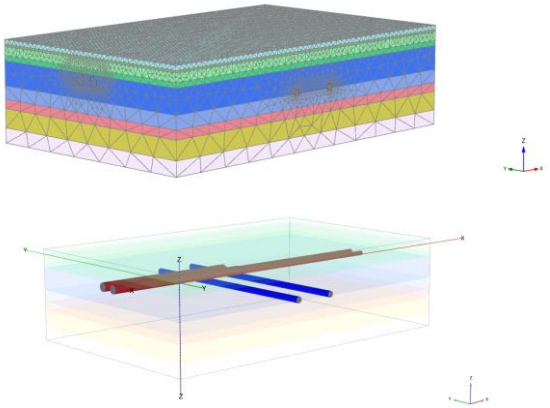

Figure 2. Images detailing model layout and geometry (NL tunnels shown in red and JLE tunnels shown in blue)

Regarding the boundary conditions, displacements at the bottom of the model were restrained in all directions. Additionally, displacements normal to the vertical boundaries of the model were restrained. The analyses involved fully-coupled consolidation and therefore required hydraulic boundary conditions to be defined. LC and LG materials were consolidating layers whereas the remaining layers were assumed to be draining. The pore water pressures in the vertical boundaries of the model as well as between the consolidating and draining layers were kept constant throughout the analyses.

Borehole data was compared against qualitative characterisations given in Hight et al. (2003) to demarcate London Clay subgroups LCB, LCA3 and LCA2. These boundaries were used in the analyses and correlate well with changes in underdrainage, K_0 and soil stiffnesses presented in Hight et al. (1993; 2003) and Yimsiri (2001). Regarding the input K_0 profile, constant values were adopted within each layer and are presented in Figure 3. The high and low K_0 magnitudes

represent typical upper and lower bound values at the top of London Clay LCA3 and LCA2.

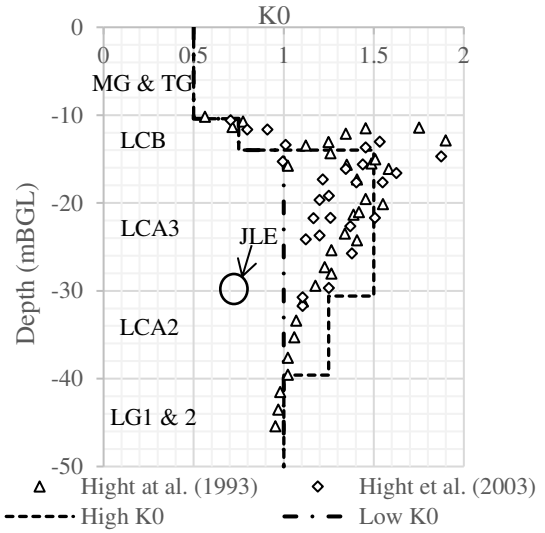

Figure 3. K_0 profile model inputs

Figure 4 presents the initial pore water pressure profile adopted in the analyses along with the measurements and estimated profile presented in Hight et al. (1993). The permeability values of each consolidating layer were adjusted for them to be compatible with the initial pore pressure field and are presented in Figure 4.

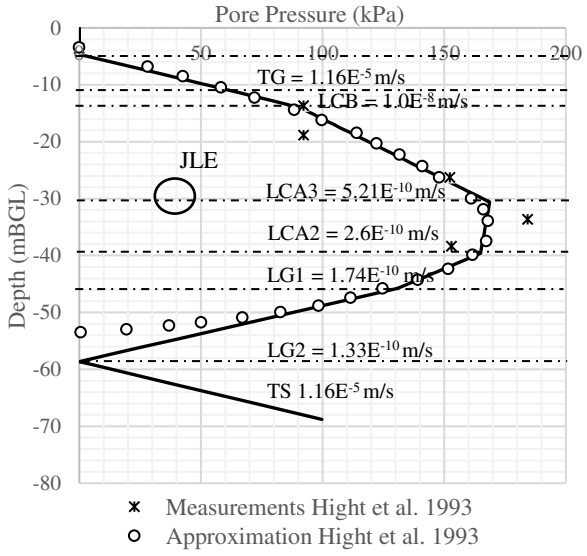

Figure 4. Calibrated underdrained pore water pressure profile

3.2 Soil constitutive modelling

The nonlinear stiffness degradation model proposed by Taborda et al. (2016) was adopted along with the Mohr-Coulomb failure criterion for the TG, LC and LG units. These models were implemented as user-defined subroutines in PLAXIS 3D (Taborda et al., 2022). Materials MG and TS were simulated as linear elastic along with the Mohr-Coulomb failure criterion. Table 1 presents the elastic modulus E and Poisson's ratio ν of the latter two materials as well as the unit weight γ and parameters for the Mohr-Coulomb criterion (cohesion c', friction angle φ' and dilatancy angle ψ') for all materials.

Table 1. Elastic and Mohr-Coulomb input parameters

Unit ID	γ (kN/m^3)	E (kPa)	ν	φ' (º)	c' (kPa)	ψ' (º)
MG	19	10E^4	0.2	30	1	12.5
TG	20	See Tables 2 and 3 for model stiffness inputs		35	0	17.5
LCB	20			23	5	11.5
LCA3	20			25	10	11.5
LCA2	20			25	15	12.5
LG1	22			27	11	11
LG2	22			27	11	11
TS	22	30E^4	0.2	32	0	16

The shear and bulk stiffness degradation parameters for the TG, LC and LG are presented in Table 2 and Table 3, respectively. The reader is referred to Taborda et al. (2016) for a detailed description of the mathematical formulation of the nonlinear stiffness model. Stiffness degradation data presented in Hight at al. (1993) for the TG material was used for calibration. Furthermore, the input parameters for LC soils were calibrated against high quality triaxial testing data published in Yimsiri (2001), on samples taken from Kennington. LG soils were assumed to follow the same stiffness degradation behaviour as materials LCA3 and LCA2.

Table 2. Input shear stiffness degradation parameters (p'_{ref} taken as 100 kPa)

Unit ID	G_0 (kPa)	a_0	b	R_{Gmin}	G_{min} (kPa)
TG	52.4E^3	2.1E^{-4}	1.25	0.1	2000
LCB	37.5E^3	1.9E^{-4}	0.925	0.1	2667
LCA3 to LG2	25.0E^3	5.85E^{-4}	0.9	0.075	2667

Table 3. Input bulk stiffness degradation parameters (p'_{ref} taken as 100 kPa)

Unit ID	K_0 (kPa)	r_0	s	R_{kmin}	K_{min} (kPa)
TG	50.0E^3	1.3E^{-4}	1.34	0.1	5000
LCB	75.0E^3	2.5E^{-5}	0.75	0.12	
LCA3 to LG2	48.0E^3	2.5E^{-5}	0.8	0.14	

3.3 Properties of tunnel linings

A thickness of 450mm corresponding to the total thickness of the primary and secondary linings was adopted for the JLE tunnels. As this study was concerned with NL tunnel displacements, accounting for the segmental nature of the JLE tunnels was considered unnecessary. Regarding the concrete properties of the JLE tunnel linings, an elastic modulus of 30GPa, a Poisson's ratio of 0.2 and a unit weight of 24kN/m^3 were adopted.

For the NL tunnels, reduced circumferential and longitudinal stiffnesses were considered to account for the segmental nature of GCI linings. The bending stiffness reduction factors in the circumferential direction ŋ and the longitudinal direction ξ are presented in Equations 1 and 2. These are defined as the ratios of the bending stiffness *EI*, in each direction, of a jointed tunnel lining over that of a continuous tunnel lining.

$$ŋ = \frac{(EI)_{C,jointed}}{(EI)_{C,continuous}} \quad (1)$$

$$ξ = \frac{(EI)_{I,jointed}}{(EI)_{I,continuous}} \quad (2)$$

The ratio ŋ was adopted as 0.77 which corresponds to the global reduction factor derived by Ruiz López et al. (2022) for a 1% tunnel ovalisation. A ratio of ξ equalling 0.11 was used (Yu et al., 2019). Bending stiffness values for the station and running tunnels are presented in Table 4. An elastic modulus of 100GPa, Poisson's ratio of 0.26 and unit weight of 70kN/m^3 was adopted for GCI.

Table 4. Input lining stiffness parameters of the NL tunnels

Tunnel ID	Material Stiffness (GPa)	Jointed (kNm^2/m)	
		ŋ.*EI*	ξ.*EI*
Station	100	16640	2378
Running		3526	504

The same bending stiffness reduction factors were assumed to be applicable to reduce the shear stiffness values which are presented in Table 5. Shear moduli G_{13} and G_{23} were calculated from elastic moduli $ξE$ and $ŋE$, respectively, and the adopted Poisson's ratio. Conversely, G_{12}, which is the in-plane shear modulus, was assumed to be unaffected by the joints and it was determined from the actual elastic modulus.

Table 5. Input shear stiffness parameters of the NL tunnels

Tunnel ID	G_{12} (kPa)	G_{13} (kPa)	G_{23} (kPa)
Station & Running	39.68E^6	4.365E^6	30.56E^6

3.4 Analysis procedures and sequence

Both NL and JLE excavations were simulated assuming undrained conditions. To reduce the computational time, excavation of the NL tunnels was conducted in a single phase, whilst applying a radial perpendicular isotropic pressure against the internal circumference. This procedure is somewhat equivalent to the tunnel excavation performed in 2D plane strain analyses, where deconfinement magnitudes are specified. For the station and running tunnels, an internal pressure of 120kPa and 90kPa respectively was applied. For the transition between the station and running tunnels an internal pressure of 107.5kPa was applied. The NB tunnel was constructed first followed by the SB tunnel. Following tunnel excavation, the tunnel lining installation was completed by activating the shell elements representing the lining and deactivating the internal pressure. The model phases implemented for the NL tunnel construction is presented in Figure 5. A 71-year period between the NL and JLE tunnel construction was simulated with a fully coupled flow deformation analysis.

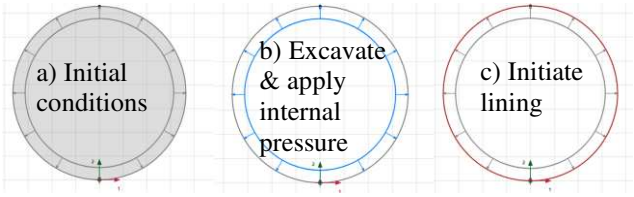

Figure 5. NL tunnel simulation

The JLE tunnels were excavated following a step-by-step approach (Katzenbach and Breth, 1981) adopting a 3m unsupported length. A bench-invert excavation with the following sequence was conducted: the top bench was first removed (Fig 6.b) followed by simultaneous excavation of the invert and installation of the upper lining (Fig 6.c). The sequence was completed by installing the lower lining (Fig 6.d). The JLE EB tunnel was driven with a delay of approximately 18m with respect to the WB tunnel.

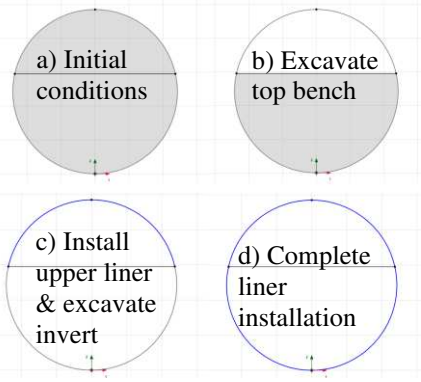

Figure 6. JLE step-by-step simulation

4 RESULTS AND DISCUSSION

Measurements of vertical displacements along the NL tunnel inverts were compared against field measurements (Standing and Selman, 2001) following completion of the JLE construction. The empirical methods based on Mair et al. (1993) for subsurface displacements have also been presented and compared against model predictions. A volume loss of approximately 1% is used and assumed typical of what was observed and targeted during the works. The empirical estimations

have been superimposed to provide an estimation of settlement shape. The results are presented in Figure 7 and Figure 8.

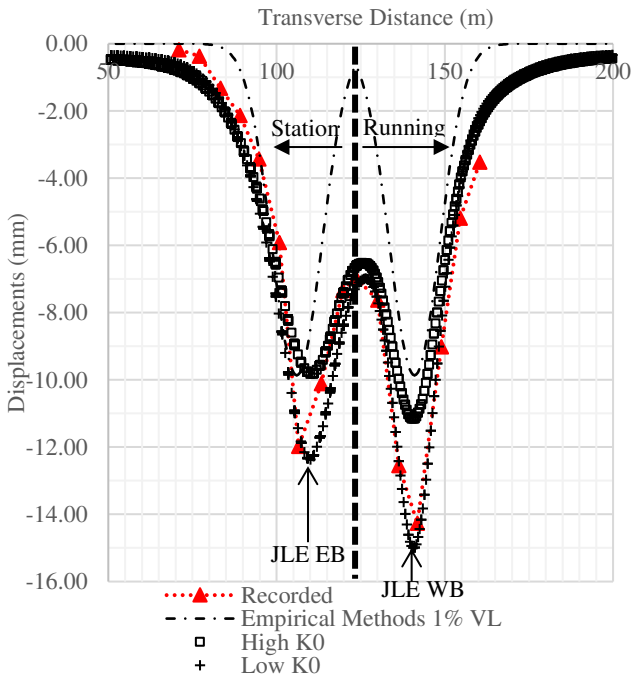

Figure 7. Vertical displacement estimations along NL NB tunnel invert

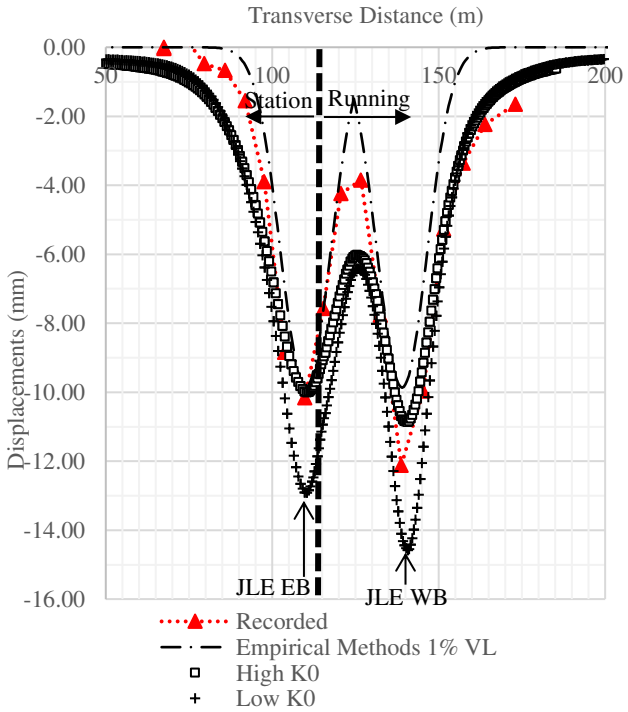

Figure 8. Vertical displacement estimations along NL SB tunnel invert

The settlement profile observed in the field was asymmetric, with magnitudes typically lower along the station tunnels compared to the running. This, as suggested by Standing and Selman (2001), may reflect the greater stiffness of these tunnels in comparison to the running tunnels. The NB tunnel settlements were also noted to be larger than those measured along the SB tunnels. Such differences in the response of the two tunnels are somewhat unexpected and might be due to differences in workmanship.

When comparing the settlement profiles against the high K_0 predictions, good estimates along the SB tunnel were obtained. For the NB tunnel, the model underestimated displacements by about 3mm. For the low K_0 soil model, good predictions were obtained for the NB tunnel; for the SB tunnel, the model overestimated displacements by approximately 3mm.

The asymmetric shape was captured in both high and low K_0 models. Larger displacements predicted along the running tunnels when compared to the station tunnels reflect the tunnel stiffness contrasts as noted in Standing and Selman (2001). Additionally, the soil stiffness degradation caused by JLE WB tunnel construction, which was excavated first, lead to additional displacements during EB tunnel construction which further enhanced the asymmetric shape.

Neither of the analyses were able to capture the differences in settlement magnitudes observed between the NB and SB tunnels. As discussed previously, these differences are possibly associated with onsite workmanship and/or soil variability and as a result, would not be captured in the current numerical simulations.

When comparing predictions given by the empirical framework against model estimates, the maximum settlements are slightly less than those given by the high K_0 analysis. As the empirical framework is limited to assuming a volume loss and greenfield displacements, it is therefore unable to capture the asymmetric tunnel response. Only an advanced numerical analysis, where the stiffening effect caused by the existing tunnels and soil stiffness degradation can be accounted, can reproduce the asymmetry of the settlement trough.

5 CONCLUSIONS

The construction of the JLE tunnels underneath the NL tunnels at the WIT site has been simulated numerically with an advanced 3D model. The numerical results were generally in good correspondence with the field measurements. This suggests that the methods adopted in this paper are adequate to simulating the interaction between new and existing tunnels. In particular, using a reduced tunnel lining stiffness to account for the presence of joints in the existing tunnels can be an appropriate strategy to obtain accurate estimations of displacements. The effect of adopting high and low K_0 profiles was considered. Neither of the two profiles evidently gave better results, with each of the analyses providing the best match with respect to the displacements of one of the existing tunnels. The numerical predictions represented the overall response of the existing tunnels more accurately than the predictions of the empirical framework.

Further investigations might consider how the transverse isotropic stiffness of London Clay affects estimations of movements on existing tunnels.

6 REFERENCES

Addenbrooke, T. I., Potts, D. M. 2001. *Building Response to Tunnelling - Chapter 12,* Thomas Telford, London.

Addenbrooke, T. I., Potts, D. M. 1996. Twin tunnel construction - Ground movements and lining behaviour. *Geotechnical Aspects of Underground Construction in Soft Ground* (Eds: Mair, R. J. & Taylor, R. N.), 441-446. Balkema, Rotterdam.

Avgerinos, V., Potts, D. M., Standing, J. R. 2017. Numerical investigation of the effects of tunnelling on existing tunnels, *Géotechnique* **67,** 808-822.

Bentley. 2022. PLAXIS Geotechnical Software, V22 (22.2.0.1078).

Franzius, J. N., Potts, D. M., Burland, J. B. 2005. The influence of soil anisotropy and K_0 on ground surface movements resulting from tunnel excavation, *Géotechnique* **55,** 189-199.

Guedes de Melo, P. F. M., Pereira, C. S. 2000. The role of the soil k_0 value in numerical analysis of shallow tunnels. *Geotechnical Aspects of Underground Construction in Soft Ground* (Eds: Kusakabe, O., Fujita, K. & Miyazaki, Y.), 379-384. Balkema, Rotterdam.

Hight, D. W., Higgins, K. G., Jardine, R. J., Potts, D. M., Pickles, A. R., De Moor, E. K., Nyirenda, Z. M. 1993. Predicted and measured tunnel distortions associated with construction of Waterloo International Terminal. *Predictive Soil Mechanics* (Eds: Houlsby, G. T. & Schofield, A. N.)*,* 317-388. Thomas Telford, London.

Hight, D. W., McMillan, F., Powell, J. J. M., Jardine, R. J., Allenou. C. P. 2003. Some characteristics of London Clay. *Characterisation and Engineering Properties of Natural Soils* (Eds: Tan, T. S., Phoon, K. K., Hight, D. W. & Leroueil, S.)*,* 851-908. Swets & Zeitlinger*,* Lisse.

Katzenbach, R., Breth, H. 1981. Nonlinear 3-D Analysis for NATM in Frankfurt Clay. *Proceedings of the 10th international conference of Soil Mechanics and Foundation Engineering,* 315-318. Balkema.

Liu, H. Y., Small, J. C., Carter, J. P., Williams, D. J. 2009. Effects of tunnelling on existing support systems of perpendicularly crossing tunnels, *Computers and Geotechnics* **36**, 880-894.

Mair, R. J., Taylor, R. N., Bracegirdle, A. 1993. Subsurface settlement profiles above tunnels in clays, *Geotechnique* **43,** 315-320.

Mair, R. J., Taylor, R. N. 1997. Theme lecture: Bored tunnelling in the urban environment. *Proceedings of the 14th International Conference on Soil Mechanics and Foundation Engineering,* 2353-2385. Balkema, Rotterdam.

Peck, R. B. 1969. Deep Excavations and Tunnelling in Soft Ground. *Proceedings of the 7th International Conference of Soil Mechanics and Foundation Engineering,* 225-290. Mexico City.

Ruiz López, A., Tsiampousi, A., Standing, J. R., Potts, D. M. 2022. Numerical investigation of a segmental grey cast iron tunnel ring: validation with laboratory data and application to field conditions, *Computers and Geotechnics* **141**, 1-19.

Standing, J. R., Selman, R. 2001. *Building Response to Tunnelling - Chapter 29*, Thomas Telford, London.

Stewart, M. 2022. 3D Numerical Modelling of Tunnel Interaction in London Stratigraphy – Jubilee & Northern Line Tunnel Case Study at Waterloo International Terminal, *MSc Thesis,* Imperial College London.

Taborda, D. M. G., Kontoe, S., Tsiampousi, A. 2022. IC MAGE IC MAGE Model 01 – strain hardening/ softening Mohr-Coulomb failure criterion with isotropic small strain stiffness (Version 2.0). Zenodo. Doi: 10.5281/zenodo.7565062.

Taborda, D. M. G., Potts, D. M., Zdravković, L. 2016. On the assessment of energy dissipated through hysteresis in finite element analysis, *Computers and Geotechnics* **71,** 180–194.

Yimsiri, S. 2001. Pre-failure deformation characteristics of soils: anisotropy and soil fabric, *PhD Thesis,* Cambridge University.

Yu, H., Cai, C., Bobet, A., Zhao, X., Yuan, Y. 2019. Analytical solution for longitudinal bending stiffness of shield tunnels, *Tunnelling and Underground Space Technology* **83**, 27-34.